

Complex transport behavior accompanying domain switching in $\text{La}_{0.1}\text{Bi}_{0.9}\text{FeO}_3$ sandwiched capacitors

R. L. Gao, Y. S. Chen, J. R. Sun, Y. G. Zhao, J. B. Li et al.

Citation: *Appl. Phys. Lett.* **101**, 152901 (2012); doi: 10.1063/1.4757987

View online: <http://dx.doi.org/10.1063/1.4757987>

View Table of Contents: <http://apl.aip.org/resource/1/APPLAB/v101/i15>

Published by the [American Institute of Physics](#).

Related Articles

Interface engineering between metal electrode and GeO_2 dielectric for future Ge-based metal-oxide-semiconductor technologies

Appl. Phys. Lett. **101**, 201601 (2012)

Non-planar substrate effect on the interface trap capacitance of metal-oxide-semiconductor structures with ultra thin oxides

J. Appl. Phys. **112**, 094502 (2012)

Gate stack dielectric degradation of rare-earth oxides grown on high mobility Ge substrates

J. Appl. Phys. **112**, 094501 (2012)

Leakage current asymmetry and resistive switching behavior of SrTiO_3

Appl. Phys. Lett. **101**, 173507 (2012)

An accurate characterization of interface-state by deep-level transient spectroscopy for Ge metal-insulator-semiconductor capacitors with $\text{SiO}_2/\text{GeO}_2$ bilayer passivation

J. Appl. Phys. **112**, 083707 (2012)

Additional information on *Appl. Phys. Lett.*

Journal Homepage: <http://apl.aip.org/>

Journal Information: http://apl.aip.org/about/about_the_journal

Top downloads: http://apl.aip.org/features/most_downloaded

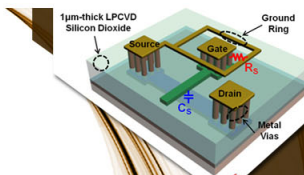
Information for Authors: <http://apl.aip.org/authors>

ADVERTISEMENT



**EXPLORE WHAT'S
NEW IN APL**

SUBMIT YOUR PAPER NOW!



SURFACES AND INTERFACES

Focusing on physical, chemical, biological, structural, optical, magnetic and electrical properties of surfaces and interfaces, and more...



ENERGY CONVERSION AND STORAGE

Focusing on all aspects of static and dynamic energy conversion, energy storage, photovoltaics, solar fuels, batteries, capacitors, thermoelectrics, and more...

Complex transport behavior accompanying domain switching in $\text{La}_{0.1}\text{Bi}_{0.9}\text{FeO}_3$ sandwiched capacitors

R. L. Gao,¹ Y. S. Chen,^{1,a)} J. R. Sun,^{1,b)} Y. G. Zhao,² J. B. Li,¹ and B. G. Shen¹

¹Beijing National Laboratory for Condensed Matter Physics and Institute of Physics, Chinese Academy of Science, Beijing 100190, China

²Department of Physics and State Key Laboratory of Low-Dimensional Quantum Physics, Tsinghua University, Beijing 100084, China

(Received 23 July 2012; accepted 25 September 2012; published online 8 October 2012)

Polarization-modulated resistive switching and fatigue behaviors of the $\text{Ag}/\text{La}_{0.1}\text{Bi}_{0.9}\text{FeO}_3/\text{La}_{0.7}\text{Sr}_{0.3}\text{MnO}_3$ capacitors have been investigated. The device resistance is found to show a V-shaped dependence on poling voltage, and the lowest resistance appears at the voltage corresponding to the coercive field of $\text{La}_{0.1}\text{Bi}_{0.9}\text{FeO}_3$. Based on this relation, three distinct resistance states can be achieved by applying appropriate pulse trains, which manifests a potential application in high-density storage technology. The fatigue properties of the sample under repeated bipolar or unipolar pulses were further analyzed. Bipolar pulses enhance the rectifying characters of the current-voltage relation, whereas unipolar pulses produce a reverse effect. Based on impedance analysis, we propose the formation of leakage paths along conductive domain walls, and it is the domain reconstruction during repeated polarization flipping that results in the complex transport behavior observed. © 2012 American Institute of Physics. [<http://dx.doi.org/10.1063/1.4757987>]

As a room temperature multiferroic, bismuth ferrite BiFeO_3 (BFO) has attracted great attention in the past few years due to its potential application in spintronics, photo-electronic, and micro-electromechanical devices.^{1–6} In addition to large ferroelectric polarization ($\sim 110 \mu\text{C}/\text{cm}^2$), diverse behaviors have been observed in BFO, such as the activation type conduction of the ferroelectric domains walls formed between 109° and 180° oriented domains,^{7,8} magnetic domain switching triggered by electric field,⁹ and giant photovoltage yielded by laser illumination.^{5,10} A combination of BFO with a secondary material also leads to distinctive phenomena, for example, the magnetic exchange bias modified by electric field in the BFO/manganite heterostructure and the rectifying behavior varied with polarization in the BFO/metal heterojunctions.^{11–15} The latter is especially interesting due to its potential application in the non-volatile memory technology and, therefore, has attracted great attention. In 2009, Choi *et al.* reported the switchable rectifying behavior in the Au/BFO/Au sandwich when the polarization direction of BFO is reversed.⁵ Changes of Schottky barrier at the metal/BFO interface accompanying the polarization reversion were proposed as the origin of this phenomenon.^{15–19} By monitoring the transient current during polarization switching, Jiang *et al.* gave the firm evidence that the rectifying switching occurred accompanying polarization changes.¹⁶ Recently, Yi *et al.* found that the polarization flipping is not enough to reverse the diode direction, and the effects of oxygen vacancies in interface layer must be considered.¹⁷

In the previous work, the BFO sandwiched samples were considered only in fully upward or fully downward polarized state (DPS), and the relation between polarization and rectifying characteristics were not established for intermediately

polarized states. Furthermore, defect migration and redistribution usually occur simultaneously with domain flipping.¹⁷ The entanglement of these effects may lead to unusual transport behavior or other unique phenomena that need to be considered for the practical application of the BFO devices. Based on these considerations, in this letter, the polarization-modulated resistive switching and the fatigue characters of the $\text{Ag}/\text{La}_{0.1}\text{Bi}_{0.9}\text{FeO}_3$ (LBFO)/ $\text{La}_{0.7}\text{Sr}_{0.3}\text{MnO}_3$ (LSMO) capacitors were systematically investigated. We demonstrated the complex dependence of current-voltage (I - V) relations on polarization state and the recyclable fatigue phenomenon under bipolar or identical pulses.

LBFO films were prepared by the pulsed laser deposition technique with the ceramic target of $\text{La}_{0.1}\text{Bi}_{0.9}\text{FeO}_3$ (10% excess Bi was introduced to compensate the sintering loss). La was incorporated to reduce leakage current.²⁰ As bottom electrode (BE), a LSMO layer (30 nm in thickness) was first deposited on (001)- SrTiO_3 (STO) substrate at the temperature of 700°C under the oxygen pressure of 50 Pa, then a 500 nm LBFO film was grown on the LSMO layer under the conditions of 650°C and 15 Pa. After deposition, the film was slowly cooled to room temperature ($2^\circ\text{C}/\text{min}$) in the oxygen atmosphere of 100 Pa, and Ag disks, 200 μm in diameter, were deposited as top electrodes (TEs) under the vacuum condition of 10^{-4} Pa. Voltage biases were applied to the Ag disks with LSMO being grounded for electric measurements. Similar to reported results,¹¹ only the (00 l) ($l = 1, 2, 3$) reflections of LBFO and STO were detected in the 2θ range from 20° to 80° by x-ray diffraction (the diffraction peaks of the LSMO film were not observed due to the thick LBFO overlayer). The full width at half maximum of the rocking curve of (002) peak is $\sim 0.6^\circ$, slightly narrower than reported values.¹¹ These results indicate an epitaxial growth of the LBFO film. Atomic force microscope analysis shows the grain size of ~ 200 nm and the surface roughness of ~ 10 nm. The out-of-plane domain structure of the

^{a)}E-mail: yschen@aphy.iphy.ac.cn.

^{b)}E-mail: jrsun@iphy.ac.cn.

non-etched LBFO film is shown in Fig. 1(a), and the dark and bright areas correspond to downward and upward poled domains, respectively.

To trace the evolution of polarization flipping under electric pulses, the so called positive-up-negative-down (PUND) method was adopted.²¹ As shown in Fig. 1(b), the transient current (I_{sw}) yielded by polarization switching was measured by the voltage on an in-series resistor of 100 Ω . The remanent polarization (P_r) was quantified by the area below the I_{sw} - t curve, divided by electrode area. The LBFO film was first driven to the fully DPS by a positive pulse of 40 V (pulse width = 12 μ s) then to an intermediate state by a negative pulse (V_{pulse}) with the amplitude between 0 and 40 V. By repeating this procedure, an arbitrary intermediate state between the fully DSP and the fully upward state (UPS) can be obtained. As shown in Fig. 1(c), the transient current first jumps to a peak value and then quickly decays to zero. Increasing poling voltage, the current peak grows and the switching time reduces. Fig. 1(d) presents the evolution of the polarization of LBFO with poling voltages. A zero-polarization state (ZPS), in which half domains are upwards poled and half domains are downwards poled, is obtained around the coercive voltage (~ 20 V).

After each pulse train, the I - V relations were measured to check the transport property of each state. Unexpected, the I - V characteristics display a complex variation with poling voltage. As shown in Fig. 2(a), the I - V curve is relatively flat in the initial DPS, gradually bends as V_{pulse} increases from 0 to -20 V, and flats again when V_{pulse} exceeds -20 V. Correspondingly, the effective resistance of the device (R), read at -4 V, experiences first a rapid drop from $\sim 2.7 \times 10^9 \Omega$ to $\sim 7.5 \times 10^7 \Omega$ then a gradual upturn from $\sim 7.5 \times 10^7 \Omega$ to $\sim 1.7 \times 10^8 \Omega$. The resistive minimum occurs at the coercive voltage of -20 V, where the device is just in the ZPS. This phenomenon was observed not only in

the process for the DPS to UPS flipping but also in the reverse process. The resistances corresponding to the DPS, UPS, and ZPS, respectively, are definite and reproducible (Fig. 2(c)), and the resultant multi-level switching is an effect of potential application in high density storage technology. In the literature, the switching behavior of BFO-based devices was usually characterized by the resistance ratio of the DPS and UPS. Here, we show that the lowest state of such devices occurs in the ZPS instead of UPS. In general, the transport behavior of the sample is determined by the Schottky barrier formed at the LBFO/electrode interface.²² According to the previous work, ferroelectric polarization will affect interfacial barrier following the relation $\Delta\phi_b = \pm P_r \delta / \epsilon_0 \epsilon_{st}$, where δ is the separation between surface polarization charge and electrode and ϵ_{st} is the static dielectric constant.²³ Based on this analysis, ϕ_b should demonstrate a monotonic variation with P_r . This actually implies a monotonic curve bending of the negative (or positive) branch of the I - V curves. The complex R - P_r relation indicates that the polarization switching-induced variation may not be limited to interfacial barrier.

To elucidate the underlying physics of the V-shaped R - V relation, a fatigue test was performed for the Ag/LBFO/LSMO device. It is found that pulses with alternative polarities (bipolar pulses) cause a great change in I - V characteristics though remnant polarization only slightly varies (see below). As shown in Fig. 3(a), the I - V relation treated by repeated ± 40 V pulses displays an increasing curve bending with the number of bipolar pulses. The double logarithmic plot in the inset of Fig. 3(a) shows a linear variation of the device resistance with switching cycles. R decreases from the initial value $\sim 6.9 \times 10^7 \Omega$ to $\sim 1.2 \times 10^7 \Omega$ after 100 cycles, $\sim 3.9 \times 10^6 \Omega$ after 1000 cycles, and $\sim 2.7 \times 10^6 \Omega$ after 5000 cycles. On the contrary, a pulse train with identical polarity (unipolar pulses) produces a reverse effect, making the

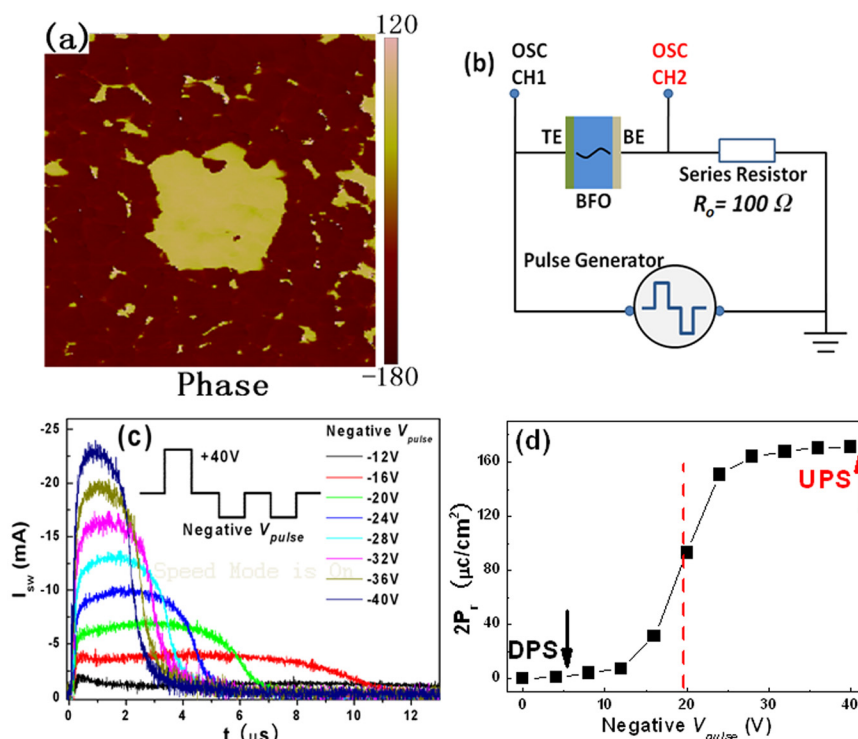


FIG. 1. (a) Out-of-plane domain structure of the non-etched LBFO surface successively poled by positive bias (large square, $2 \mu\text{m} \times 2 \mu\text{m}$) and negative bias (center square, $0.5 \mu\text{m} \times 0.5 \mu\text{m}$). (b) Experiment setup for the polarization switching by electric pulses. (c) Time dependence of the switching current with varied negative V_{pulse} . (d) $2P_r$ - V_{pulse} curve derived from the transient current.

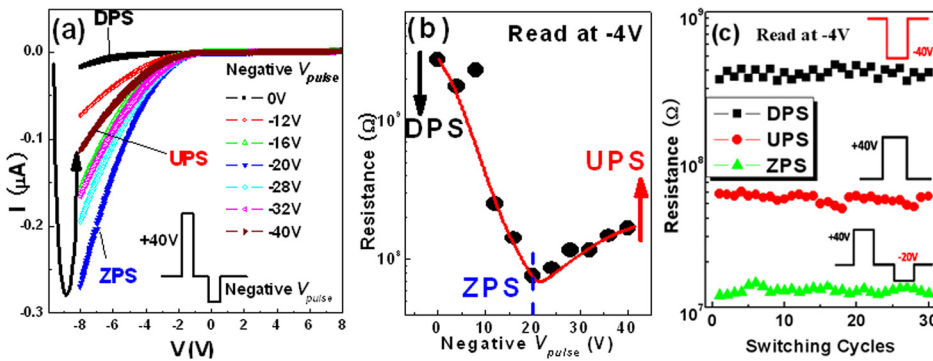


FIG. 2. (a) I - V curves measured at each intermediate polarization state. (b) R - V_{pulse} curve with a minimal value at coercive voltage. (c) Resistance distributions of the DPS, UPS, and ZPS poled by the inset pulse trains.

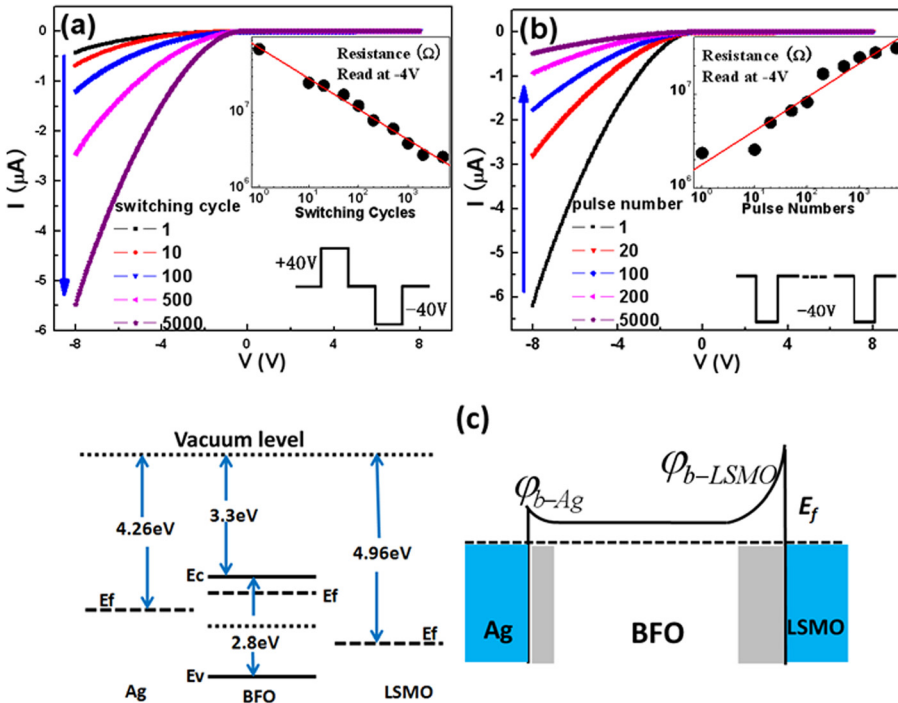


FIG. 3. I - V curves measured after the treatments of ± 40 V alternative pulses (a) and ± 40 V identical pulses (b). Inset: Resistance (read at -4 V) dependence on switching cycles or pulse numbers. (c) Band diagram of the Ag/LBFO/LSMO device.

bent curves flat again (Fig. 3(b)). For example, applying 5000 successive pulses (-40 V in magnitude) to the UPS resulted by the bipolar fatigue, the resistance returns from $\sim 2.4 \times 10^6 \Omega$ to $\sim 3.0 \times 10^7 \Omega$. By selecting the polarity of the end pulse in pulse trains, the sample can be driven to either the UPS or the DPS. However, the general tendency for the I - V curves towards bending/flattening is unaffected while repeating alternative/identical pulses.

Based on the work functions of Ag, LSMO (4.26 eV, 4.96 eV), and the electron affinity/band gap of BFO (3.3 eV/2.8 eV),²⁴ a band diagram can be depicted for the Ag/LBFO/LSMO device, here LBFO has been treated as an n-type semiconductor.^{25,29} As shown in Fig. 3(c), the barrier height of the LBFO/LSMO junction is higher than that of the Ag/LBFO junction, which explains why the current level is low/high under positive/negative bias. It is worth to note that positive current remains small (less than 1 nA at $+4$ V) in the fatigue process, though negative current varies by several orders of magnitude. It means that, different from the Ag/LBFO junction, the LBFO/LSMO junction is insensitive to electric pulses for some reasons.²⁶

To check what has happened in the pulse treatment process, the impedance spectra of the sample were further studied. The imaginary part of the frequency-dependent modulus

(M'') measured under -6 V is shown in Fig. 4(a). For a parallel RC circuit, the M'' should be $M'' = \frac{C_0}{C} \left(\frac{\omega RC}{1 + (\omega RC)^2} \right)$, where $\omega = 2\pi f$ is the angular frequency and C_0 is the vacuum capacitance. According to this formula, a M'' - f spectrum with only a single broad peak can be described by a single RC equivalent circuit, and the peak position and peak height have the forms of $1/RC$ and $C_0/2C$, respectively. Corresponding to the curve bending/flattening of the I - V relation, the peak position of M'' displays a high/low frequency shift. It is $\sim 1.7 \times 10^3$ Hz in the initial state, $\sim 2.0 \times 10^3$ Hz after 1000 ± 40 V pulses, and $\sim 1.4 \times 10^4$ Hz after $1000 - 40$ V pulses. The cole-cole plots of the real and imaginary impedance measured after different pulse treatments are shown in Fig. 4(b). The impedance spectra can be well fitted by one parallel RC circuit adopting a constant capacitance of 8.4 pF and different resistances, 9.8 M Ω for $1000 - 40$ V pulses and 2.45 M Ω for 1000 ± 40 V pulses. Considering the fact that the band bending of LBFO near the LBFO/LSMO interface will be flattened by the negative bias (-6 V), the impedance may be mainly contributed by the Ag/LBFO junction. With this in mind, it is understandable that the sample with two junctions can be well described by a single RC circuit. The

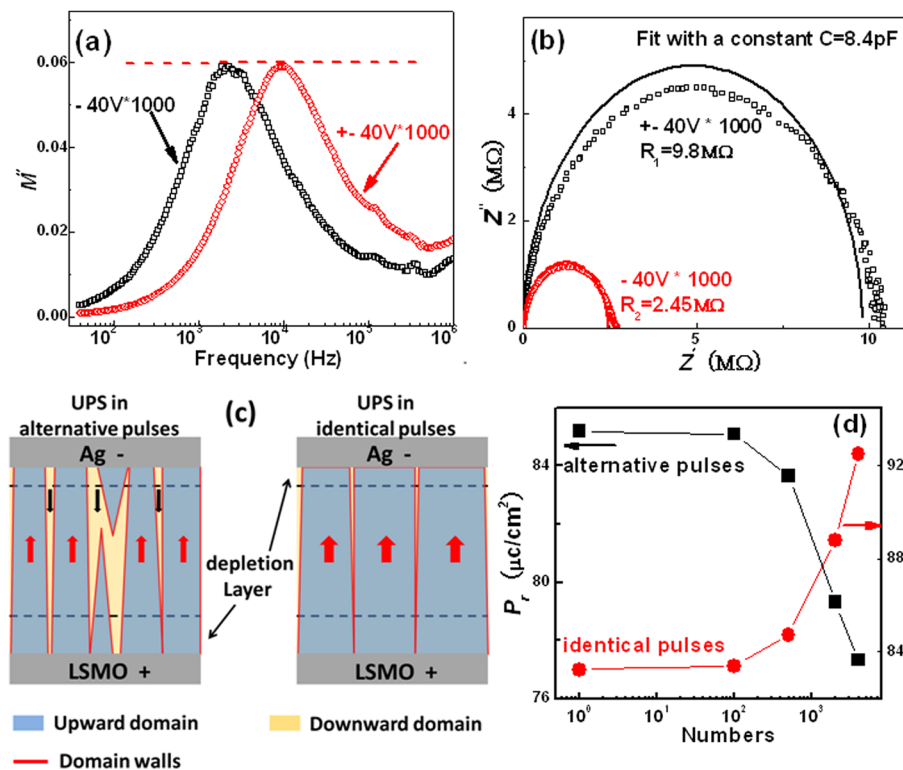


FIG. 4. (a) Frequency dependence of the electric modulus M'' (imaginary part) after the treatment by 1000 alternative pulses or 1000 identical pulses. (b) Cole-cole plots of the real and imaginary impedances. Hollow symbols are experimental data and solid lines are results of curve-fitting. (c) Schematic domain structure of the LBFO film after alternative or identical pulse treatment. Local leakage paths form along the conductive domain walls. (d) Variation of P_r under different pulse treatments.

most remarkable observation of the present work is that the peak height is essentially constant whereas the peak position changes after fatigue tests. This result implies a constant capacitance and a varied resistance. It is possible that conduction filaments are formed in the depletion layer of the Ag/LBFO junction. These leakage paths can short-circuit the interfacial barriers, thus, modify the transport property. In contrast, the capacitance of Ag/LBFO/LSMO will not be influenced since the conduction filaments essentially do not affect capacitor area.

The first thing affected by bipolar fatigue may be domain structure. In general, bipolar fatigue usually causes an attenuation of the ferroelectric domains. As reported by Lupascu and Rabe,²⁷ needle-shaped domains along the electric field direction could be formed under alternative pulses. Yang *et al.*²⁸ indicated that the bipolar fatigue would suppress the sideways domain growth, resulting in nanometer-sized one-dimensional domains. A distinctive feature of this kind of domain structure is the increased domain wall density, which may affect the transport properties of the sample. As reported for the BFO materials, oxygen vacancies preferred to locate at domain walls, forming a sub-band that facilitates electron hopping.^{7,8} The resistivity of domain walls is estimated to be five to six orders of magnitude lower than the BFO bulk. It is therefore possible for this kind of domain walls to serve as conduction filaments in Ag/LBFO (Fig. 4(c)). This explains the resistance reduction after bipolar fatigue. In contrast, domains will merge with each other under identical pulses, leading to a decrease in domain wall density, thus, a reduction in resistance.

Because of technical difficulty, we failed to directly measure the variation of the domain structures of the LBFO film during the fatigue test. However, we did observe lateral evidence for domain structure change. By monitoring the transient current yielded by polarization flip, we found a reduction up to $\sim 7\%$ in P_r after 4000 alternative pulses (Fig. 4(d)). It tallies with the appearance of tiny domains in the

LBFO film, which will not flip with pulse polarity due to enhanced domain wall pinning and reduced polarization.²⁸ We also observed a reverse process under identical pulses, which may indicate the disappearance of “dead” domains. The complex R - P_r relation in Fig. 2(b) can be understood in the same scenario. We noted that the ZPS is a special state in which ferroelectric domains are half upwards and half downwards poled. In this case, the disordered domains may share the same features with those formed under alternative pulses, and percolating conduction paths could be formed, leading to the low resistance of ZPS. Further flipping the devices with negative (positive) voltage, the upward (downward) domains will grow sideways, causing a reduction in domain wall density, and therefore, an increase in device resistance.

In summary, polarization-modulated switching behavior and fatigue phenomenon have been investigated for the Ag/LBFO/LSMO capacitors. A complex dependence of device resistance on poling voltage is observed. Based on this relation, three distinct polarization states can be obtained by selecting appropriate poling voltages, which manifests a potential application in high-density storage technology. Bipolar and unipolar electric pulses produce different effects on the transport property of the device. The former enhances the rectifying characteristics of the device, whereas the latter produces a reverse effect. Considering the domain reconstruction and the high conductivity of the domain walls of LBFO, the distinctive fatigue characters can be understood. The present work will facilitate advanced investigations on both fundamental physics and potential applications of the BFO ferroelectric.

This work has been supported by the National Basic Research of China, the National Natural Science Foundation of China, the Knowledge Innovation Project of the Chinese Academy of Sciences, and the Beijing Municipal Natural Science Foundation.

- ¹W. Eerenstein, N. D. Mathur, and J. F. Scott, *Nature* **442**, 759 (2006).
- ²R. Ramesh and N. A. Spaldin, *Nature Mater.* **6**, 21 (2007).
- ³J. Wang, J. B. Neaton, H. Zheng, V. Nagarajan, S. B. Ogale, B. Liu, D. Viehland, V. Vaithyanathan, D. G. Schlom, U. V. Waghmare, N. A. Spaldin, K. M. Rabe, M. Wuttig, and R. Ramesh, *Science* **299**, 1719 (2003).
- ⁴Y. H. Chu, L. W. Martin, M. B. Holcomb, and R. Ramesh, *Mater. Today* **10**, 16 (2007).
- ⁵T. Choi, S. Lee, Y. J. Choi, V. Kiryukhin, and S. W. Cheong, *Science* **324**, 63 (2009).
- ⁶J. Li, J. Wang, M. Wuttig, R. Ramesh, N. Wang, B. Ruetter, A. P. Pyatakov, A. K. Zvezdin, and D. Viehland, *Appl. Phys. Lett.* **84**, 5261 (2004).
- ⁷J. Seidel, L. W. Martin, Q. He, Q. Zhan, Y. H. Chu, A. Rother, M. E. Hawkrige, P. Maksymovych, P. Yu, M. Gajek, N. Balke, S. V. Kalinin, S. Gemming, F. Wang, G. Catalan, J. F. Scott, N. A. Spaldin, J. Orenstein, and R. Ramesh, *Nature Mater.* **8**, 229 (2009).
- ⁸S. Farokhipoor and B. Noheda, *Phys. Rev. Lett.* **107**, 127601 (2011).
- ⁹Q. He, C. H. Yeh, J. C. Yang, G. S. Bhalla, C. W. Liang, P. W. Chiu, G. Catalan, L. W. Martin, Y. H. Chu, J. F. Scott, and R. Ramesh, *Phys. Rev. Lett.* **108**, 067203 (2012).
- ¹⁰W. Ji, K. Yao, and Y. C. Liang, *Adv. Mater.* **22**, 1763 (2010).
- ¹¹J. Dho, X. Qi, H. Kim, J. L. MacManus-Driscoll, and M. G. Blamire, *Adv. Mater.* **18**, 1445 (2006).
- ¹²L. W. Martin, Y. H. Chu, M. B. Holcomb, M. Huijben, P. Yu, S. Han, D. Lee, S. X. Wang, and R. Ramesh, *Nano Lett.* **8**, 2050 (2008).
- ¹³H. Bea, M. Bibes, F. Ott, B. Dupe, X. H. Zhu, S. Petit, S. Fusil, C. Deranlot, K. Bouzehouane, and A. Barthelemy, *Phys. Rev. Lett.* **100**, 017204 (2008).
- ¹⁴H. Yang, H. M. Luo, H. Wang, I. O. Usov, N. A. Suvorova, M. Jain, D. M. Feldmann, P. C. Dowden, R. F. DePaula, and Q. X. Jia, *Appl. Phys. Lett.* **92**, 102113 (2008).
- ¹⁵G. L. Yuan and J. Wang, *Appl. Phys. Lett.* **95**, 252904 (2009).
- ¹⁶A. Q. Jiang, C. Wang, K. J. Jin, X. B. Liu, J. F. Scott, C. S. Hwang, T. A. Tang, H. B. Lu, and G. Z. Yang, *Adv. Mater.* **23**, 1277 (2011).
- ¹⁷H. T. Yi, T. Choi, S. G. Choi, Y. S. Oh, and S.-W. Cheong, *Adv. Mater.* **23**, 3403 (2011).
- ¹⁸D. Lee, S. H. Baek, T. H. Kim, J.-G. Yoon, C. M. Folkman, C. B. Eom, and T. W. Noh, *Phys. Rev. B* **84**, 125305 (2011).
- ¹⁹A. Tsurumaki, H. Yamada, and A. Sawa, *Adv. Funct. Mater.* **22**, 1040 (2012).
- ²⁰A. Lahmar, S. Habouti, M. Dietze, C. H. Solterbeck, and M. Es-Souni, *Appl. Phys. Lett.* **94**, 012903 (2009).
- ²¹J. F. Scott, L. Kammerdiner, M. Parris, S. Traynor, V. Ottenbacher, A. Shawabker, W. F. Oliver, *J. Appl. Phys.* **64**, 787 (1988).
- ²²A simple estimation indicates the vertical resistance of the BFO film is only $\sim 10^4 \Omega$ (the resistivity of as-deposited BFO is $10^6 \Omega \text{mm}$ measured by the four-probe technique), while the junction resistance is larger than $10^7 \Omega$. The transport behavior of device is mainly determined by the two junctions.
- ²³L. Pintilie and M. Alexe, *J. Appl. Phys.* **98**, 124103 (2005).
- ²⁴S. J. Clark and J. Robertson, *Appl. Phys. Lett.* **90**, 132903 (2007).
- ²⁵The BFO film has been annealed in an oxygen pressure of 100 Pa, which may yield oxygen vacancies according to the work of Yuan *et al.*²⁹
- ²⁶A defective layer at the BFO/electrode interface can depress the response of interfacial barrier to polarization change as demonstrated by Ref. 19.
- ²⁷D. C. Lupascu and U. Rabe, *Phys. Rev. Lett.* **89**, 187601 (2002).
- ²⁸S. M. Yang, T. H. Kim, K. J. G. Yoon, and T. W. Noh, *Adv. Funct. Mater.* **22**, 2310 (2012).
- ²⁹G. L. Yuan, L. W. Martin, R. Ramesh, and A. Uedono, *Appl. Phys. Lett.* **95**, 012904 (2009).